ELSEVIER

Desalination 183 (2005) 341–352

DESALINATION

www.elsevier.com/locate/desal

Design and analysis of humidification dehumidification desalination process

Hisham Ettouney

Department of Chemical Engineering, Kuwait University, P.O. Box 5969, Safat 13060, Kuwait
Tel. +965 481 1188 ext. 5619; Fax +965 483 9498, −481 1772; email: hisham@kuc01.kuniv.edu

Received 7 February 2005; accepted 15 March 2005

Abstract

Humidification dehumidification desalination process is viewed as a promising technique for small capacity production plants. The process has several attractive features, which includes operation at low temperature, ability to combine with sustainable energy sources, i.e., solar, geothermal, and requirements of low level of technical features. This paper evaluates the characteristics for several layouts for the humidification dehumidification desalination process. The common feature among these processes is the air humidification tower, where the humidity of the ambient air is increased to saturation at the desired design temperature. The main difference among various layouts is the dehumidification process. The most common scheme is to use a condenser to reduce the humidified air temperature and to condense the fresh water product. Other possible layouts includes vapor compression, desiccant air drying, and membrane air drying. The design equations are developed for the humidification/condenser and the humidification/desiccant systems. Discussion and performance evaluation of various layout shows the need to fully optimize these configurations. This is necessary to obtain the best design and operating conditions that give the minimum product cost.

Keywords: Desalination; Humidification; Dehumidification; Air drying; Vapor compression

1. Introduction

Desalination research and developments of new technologies for small capacity plants is strongly hampered by the rapid progress of the reverse osmosis process (RO). Also another important factor is the use of the ever reliable and large scale multi-stage flashing desalination plants (MSF). Also, use of water distribution networks are common even for remote and small population areas. This makes development and use of new technologies highly challenging because of difficulties

*Corresponding author.

Presented at the Conference on Desalination and the Environment, Santa Margherita, Italy, 22–26 May 2005. European Desalination Society.

doi:10.1016/j.desal.2005.03.039

in applying and accepting new technologies and lack of field experience. Irrespective of these facts, the capital for MSF plants together with an intensive water distribution system is very large. Also, the RO process requires high level of technology for membrane synthesis and module preparation. In addition, feed pretreatment for the RO process is necessary and intensive in most cases.

Development and use of new technologies for small capacity plants is highly desirable. Although, preliminary prototypes and pilot scale units might not the final optimum choice. However, such attempts may prove useful on the long range, where, the much thought after efficient, reliable, and inexpensive desalination process might be partially or fully developed. The list of such techniques involve combination with various types of heat pumps for efficient energy use, adopting solar or other renewable energies, use of non-conventional construction materials, i.e., plastics and use of more efficient evaporation/condensation units.

This study focuses on conceptual design of various schemes for water desalination by the humidification/dehumidification system (HDH). Such configuration is highly valued by researchers because of its low level of technological requirements [1–13]. This design might be suitable for industrial sites as well as remote and small population regions. Careful review of previous literature studies show that a major part of these studies is focused on performance evaluation of the HDH system combined with solar energy [3,6–10,12,13]. Also, testing of a multiple effect form of this configuration is thought for increase of the system performance [5]. A novel concept that includes air humidification followed by mechanical compression is presented by Vlachogiannis et al. [11]. This configuration is reported to have very large specific power consumption, which is almost 100 times greater than that consumed by the conventional mechanical vapor compression process [14]. This drawback is caused by the need to compress a large amount of air in addition to the product vapor. Other literature studies of the HDH system includes performance evaluation [7], modeling [4,8], or correlation development for the heat and mass transfer coefficients [9].

This study presents mathematical models for the conventional HDH process. In addition two novel processes are considered. Both processes include the conventional humidification column. Air drying and recovery of the water product is made by either desiccant absorption or membrane separation.

2. Conventional HDH

Conventional HDH process is formed of three main parts, see Fig. 1(a). These are the humidifier, where the intake air humidity is increased to saturation conditions, the condenser, where the humidified air is cooled to condense the product water, and the feed seawater heater. It should be noted that the intake seawater is preheated in the dehumidification unit. Further heating of the feed seawater in the feed heater. This is necessary to achieve the desired design conditions. This is made with aid of an external heat source, for example solar collector, heating steam, diesel engine, or other forms of low grade energy.

Analysis of the conventional HDH includes design of the humidifier, condenser, and heater. Modeling of these systems assumes steady state operation and negligible losses to the surroundings. Also, it is assumed that the air stream leaving the humidifier and the condenser are saturated. The humidifier model includes the design equation for the humidifier volume and the overall energy balance. A simple model [15] is used to determine the humidifier volume. The humidifier energy balance is given by

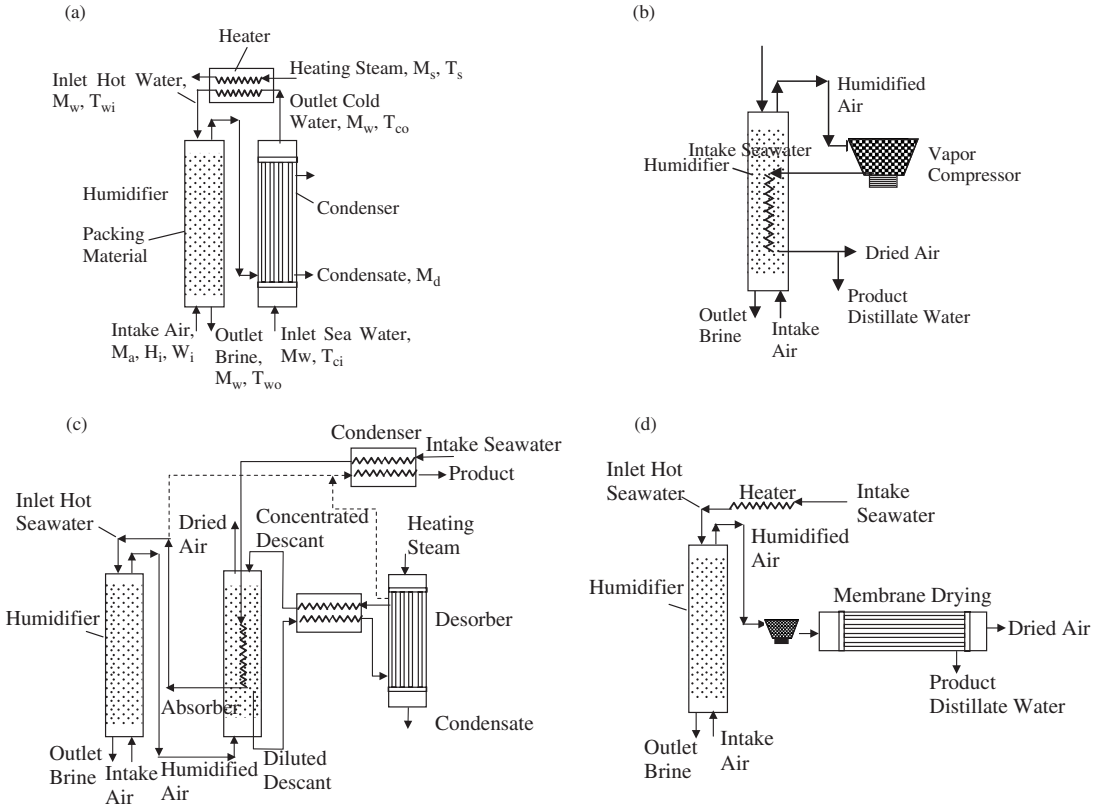

Fig. 1. (a) Conventional humidification dehumidification desalination process; (b) Humidification vapor compression; (c) Conventional humidification dehumidification desalination process; (d) Humidification and membrane drying.

$$M_{\mathrm{a}}\ (H_{\mathrm{a}_o} - H_{\mathrm{a}_i}) = M_{\mathrm{w}} Cp_{\mathrm{w}} (T_{\mathrm{w}_i} - T_{\mathrm{w}_o}) \tag{1}$$

The humidifier volume is given by the

$$Z_{\mathrm{h}} = \frac{2M_{\mathrm{w}} Cp_{\mathrm{w}} M_{\mathrm{a}}^2 (C_1 - C_2)}{C_{\mathrm{s}} K_y a_{\mathrm{h}} A_{\mathrm{h}}} \tag{2}$$

$$C_1 = ATAN((311.0344\ T_{\mathrm{w}_i} + B_1)/B_{\mathrm{s}}) \tag{3}$$

$$C_2 = ATAN((311.0344\ T_{\mathrm{w}_o} + B_1/B_{\mathrm{s}}) \tag{4}$$

$$B_{\mathrm{s}} = (622.0688\ B_{\mathrm{o}} - B_1^2)^{1/2} \tag{5}$$

$$B_o = 69344.83 - H_{\mathrm{a}_i} + M_{\mathrm{w}}\ Cp_{\mathrm{w}}\ M_{\mathrm{a}}\ T_{\mathrm{w}_o} \tag{6}$$

$$B_1 = -3689.66 - M_{\mathrm{w}}\ Cp_{\mathrm{w}}\ M_{\mathrm{a}} \tag{7}$$

Solution of Eqs. (1) and (2) requires definition of the air enthalpy, the air absolute humidity, the water latent heat, and the water specific heat. The air enthalpy is expressed in terms of the air temperature and humidity

$$H_{\mathrm{a}} = (Cp_{\mathrm{a}} + Cp_{\mathrm{v}} W)T + \lambda W \tag{8}$$

The air absolute humidity is given as a function of the atmospheric pressure and vapor pressure at the dry bulb temperature

$$W = 0.62198 \frac{p_{\mathrm{d}}}{(p_{\mathrm{atm}} - p_{\mathrm{d}})} \quad (9)$$

The water vapor pressure at the dry bulb temperature

$$p_{\mathrm{d}} = \phi p_{\mathrm{s}} \quad (10)$$

The condenser model includes the energy balance equation and the heat transfer equation between the cooling water and the air/condensing vapor stream. These two equations are given by

$$M_{\mathrm{cw}} Cp_{\mathrm{cw}} (T_{\mathrm{cw}_o} - T_{\mathrm{cw}_i}) = M_{\mathrm{a}} (H_{\mathrm{o}} - H_{\mathrm{c}}) \quad (11)$$

$$M_{\mathrm{cw}} Cp_{\mathrm{cw}} (T_{\mathrm{cw}_o} - T_{\mathrm{cw}_i}) = U_{\mathrm{c}} A_{\mathrm{c}} LMTD_{\mathrm{c}} \quad (12)$$

In Eqs. (11) and (12) the logarithmic mean temperature difference and the overall heat transfer coefficient are given by the following relations

$$LMTD_{\mathrm{c}} = \frac{(T_{\mathrm{a_c}} - T_{\mathrm{cw}_o}) - (T_{\mathrm{a_c}} - T_{\mathrm{cw}_i})}{\ln\left(\frac{(T_{\mathrm{a}_o} - T_{\mathrm{cw}_o})}{(T_{\mathrm{a_c}} - T_{\mathrm{cw}_i})}\right)} \quad (13)$$

$$\frac{1}{U_{\mathrm{c}}} = \frac{1}{h_{\mathrm{c}_i}} \frac{r_{\mathrm{c}_o}}{r_{\mathrm{c}_i}} + Rf_{\mathrm{c}} + \frac{r_{\mathrm{c}_o} \ln\left(\frac{r_{\mathrm{c}_o}}{r_{\mathrm{c}_i}}\right)}{k_{\mathrm{c}}} + \frac{1}{h_{\mathrm{c}_o}} \quad (14)$$

The production of distilled water is given by the following balance equation

$$M_{\mathrm{d}} = M_{\mathrm{a}} (W_o - W_{\mathrm{c}}) \quad (15)$$

The model of the feed water heater assumes use of saturated heating steam to increase the feed water temperature to the required design value. The heater model includes the energy balance equation and the heat transfer equation

$$M_{\mathrm{w}} Cp_{\mathrm{w}} (T_{\mathrm{w}_i} - T_{\mathrm{cw}_o}) = M_{\mathrm{s}} \lambda_{\mathrm{s}} \quad (16)$$

$$M_{\mathrm{s}} \lambda_{\mathrm{s}} = U_{\mathrm{ht}} A_{\mathrm{ht}} LMTD_{\mathrm{ht}} \quad (17)$$

In Eq. (17) the logarithmic mean temperature difference is given by

$$LMTD_{\mathrm{ht}} = \left(\frac{(T_{\mathrm{cw}_o} - T_{\mathrm{w}_i})}{\ln\left(\frac{(T_{\mathrm{s}} - T_{\mathrm{w}_i})}{(T_{\mathrm{s}} - T_{\mathrm{cw}_o})}\right)} \right) \quad (18)$$

The correlations used in the above model are extracted from reference [16]. The system model (Eqs. 1–4, 11–17) are used to design the conventional HDH desalination system. An illustration for the system design is made for a system capacity of 100 m^3/d. The intake seawater temperature is 25°C, the seawater temperature leaving the condenser is 60°C, the seawater temperature leaving the heater and entering the humidifier is 90°C, and the water temperature leaving the humidifier is 40°C. The air temperatures include the air temperature entering the humidifier, the air temperature leaving the humidifier, the air temperature leaving the condenser, which are 25, 65, and 35°C, respectively. The relative humidity of the air stream entering the humidifier, leaving the humidifier, and leaving the condenser are 10, 100 and 100%, respectively. The tube length and diameter in the condenser are equal to 10 and 0.03 m, respectively. The heating steam temperature is assumed higher than the outlet water temperature from the heat by 10°C. The cross section area of the condenser are equal to 4 m^2. The mass transfer coefficient for water vapor in air is kept constant at 0.354 kg/(s m^3) and the overall heat transfer coefficient in the condenser is also kept constant at 0.1 kW/m^2 K [9,17].

Since all of the system temperatures are selected, then, solution of the model equations is non-iterative and proceeds sequentially. Solution starts with calculations of the air stream properties, which includes the saturation pressure of the water vapor, the absolute humidity, the specific heat at constant pressure, the latent heat of water evaporation, and the enthalpy. Calculations also includes the specific heat at constant pressure for the water stream entering and leaving each of the three units. Summary of these values is shown in Table 1. The design results, which includes flow rates, area, and dimensions are also summarized in Table 1. The performance ratio for the set of conditions shown is equal to 1.23. However, achieving this relatively high value requires a very large condenser area. Also, the height of the cooling tower is large. The large condenser area is caused by the low value of the overall heat transfer coefficient. The specific value for the heat transfer area is almost 10 times great than conventional desalination systems, i.e., MSF and MEE [16]. Also, the larger humidifier length is caused by the large humidification range and temperature difference.

Table 2 shows performance summary for the HDH system as a function of the outlet air temperature. Either the lower and higher limits of the outlet air temperature gives very large humidifier height. This is because of the decrease in the driving force for heat and mass transfer. The minimum humidifier height of 12.28 m is obtained for a temperature of 55°C. On the other hand, the highest performance ratio of 1.14 is obtained at a humidifier height of 14.63 m. It should be stressed that variations in the condenser area are insensitive to variations in the outlet air temperature with values greater than 4000 m^2. Further evaluation of the results show that the flow rate ratio of the water to air varies between 0.5 and 4 as the outlet air temperature is increased. This analysis calls for

Table 1
Summary of physical properties and design properties of conventional HDH system

Property	Value	Dimensions	Design Parameter	Value	Dimensions
p_{s_i}	3.17	kPa	M_a	6.907	kg/s
p_{s_o}	25.04	kPa	M_w	16.87	kg/s
p_{s_c}	5.63	kPa	M_c	21.86	kg/s
W_i	0.0195	kg/kg	A_c	4433.4	m^2
W_o	0.204	kg/kg	$LMTD_c$	7.21	C
W_c	0.0366	kg/kg	A_t	0.94	m^2
H_i	73.74	kJ/kg	N_t	4704.03	
H_o	589.12	kJ/kg	N_r	68.59	
H_c	126.11	kJ/kg	Z_b	2.53	m
λ_i	2442.22	kJ/kg	Z_h	16.58	m
λ_o	2346.12	kJ/kg	M_s	0.94	kg/s
λ_c	2418.43	kJ/kg	PR	1.23	
λ_s	2257.25	kJ/kg K			
Cp_{a_i}	1.006	kJ/kg K			
Cp_{a_o}	1.009	kJ/kg K			
Cp_{a_c}	1.007	kJ/kg K			
Cp_{c_i}	4.186	kJ/kg K			
Cp_{c_o}	4.183	kJ/kg K			
Cp_{w_i}	4.203	kJ/kg K			
Cp_{w_o}	4.181	kJ/kg K			

Table 2
Performance summary of the HDH system as a function of the outlet air temperature from the humidifier

T_{a_o}	M_a	M_w	M_{cw}	A_c	Z_h	M_s	PR	sA
36	525.77	258	156.96	5447.18	113.83	28.28	0.04	4706.37
40	94.04	59.41	83.95	4855.66	26.94	6.07	0.19	4195.29
45	40.66	34.61	54.3	4711.44	16.41	3.21	0.36	4070.69
50	23.26	26.38	39.92	4619.58	13.3	2.2	0.53	3991.32
55	14.84	22.3	31.42	4546.75	12.28	1.66	0.7	3928.39
60	9.99	19.88	25.82	4485.67	12.54	1.29	0.9	3875.62
65	6.91	18.3	21.86	4433.44	14.63	1.02	1.14	3830.49
70	4.82	17.19	18.92	4388.42	24	0.8	1.45	3791.6
73	3.88	16.68	17.49	4364.39	250.39	0.68	1.7	3770.83

system optimization through calculations of the minimum unit product cost. Also, attempts to evaluate other configurations for water vapor condensation to reduce the heat transfer area of the condenser. This can be made through the use of other separation schemes, which are discussed in the next sections.

3. HDD—vapor compression

This system is previously proposed by Vlachogiannis et al. [11]. In this configuration, the humidified air is compressed to higher pressure. This results in simultaneous increase in the air temperature and pressure. The compressed air is then cooled against the feed seawater. This results in water vapor condensation. The system includes the conventional air humidifier and the air/vapor compressor. The system shown in Fig. 1(b) includes simultaneous heating of the humidifier air and water streams through exchange of heat with the compressed humidified air stream. This setup might be modified through the use of a separate water preheater (water vapor condenser) system as in the conventional HDH system. This might be more technically feasible, since the air humidification unit and the water vapor condenser are not a specially designed system as in the unit shown in Fig. 1(b).

The main drawback of the mechanical vapor compression approach is the need to compress a large amount of air together with the water vapor. This is just about the same as in the conventional HDH process, where the air presence together with the water vapor have a dramatic effect on the overall heat transfer coefficient. For condensation of pure water vapor, the overall heat transfer coefficient may vary over a range of 2–4 kW/m^2 K. On the other hand, the overall heat transfer coefficient for water condensation in presence of air is in the order of 0.1 kW/m^2 K. Therefore, compression of a large amount of air together with a small amount of water vapor results in a specific power consumption close to 200 kWh/m^3 [11]. This is extremely large when compared against the power consumption of the RO process or the single effect mechanical vapor compression, with values ranging from 5 to 15 kWh/m^3 [16].

4. Humidification desiccant absorption

The humidification process combined with desiccant material may involve use of a liquid desiccant, i.e., lithium bromide solution, or a solid desiccant, i.e., zeolite. The adsorption process is unsteady; therefore, it is necessary to use two solid beds. In this case one of the

two beds will be operated for the adsorption process, while the second will go through regeneration or water vapor desorption. The main feature of the absorption/adsorption processes is the generation of a large amount of heat, which can be used for preheating of the feed water. Desiccant regeneration would require use of an external heating source, which might be heating steam or a diesel engine. The main merit of this process is its proven high efficiency [18–21]. However, a main drawback might be the lack of field experience in design, operation, and maintenance of the desiccant absorption units. Also, it is evident from the process diagram, see Fig. 1(c), is the need to operate a large number of units, which includes air humidifier, absorption/adsorption bed, regeneration unit, desiccant heat exchanger, and water vapor condenser.

The air humidifier is similar to that of the convention humidification process. The absorber/adsorption units are quiet elaborate, where the humidified air stream is passed through the desiccant material. For liquid desiccant this process might involve use of packed or tray tower to improve the absorption efficiency. For the adsorption process use of a solid packed bed is the common choice. It should be noted that the intake seawater gains part of its heating by passing through the absorption/adsorption bed. In this case, the seawater will gain the heat generated during the absorption process. Also, part of the distillate fresh water product is formed during this heating process. The diluted liquid desiccant or the exhausted solid desiccant then exchanges heat with the concentrated liquid desiccant. This is necessary to reduced the amount of heating steam and to improve the process efficiency. The regeneration process is achieved by heating steam or other external heating source. This results in water evaporation and drying of the solid desiccant or increasing the concentration of the liquid desiccant. The water vapor generated during this process forms the product stream. This requires use of the cold intake seawater to condensate the water vapor.

Analysis of this process requires design of the air humidifier, the absorption unit, the regeneration unit, heat exchanger, and the vapor condenser. The design case study is applied to lithium bromide desiccant. Design of the air humidifier is similar to that of the conventional humidification system. Assumptions used in the model development include steady state operation and negligible heat losses from various units to the surroundings. The regeneration and absorption units are assumed to operate at isothermal conditions, i.e., the inlet and outlet temperatures of the desiccant stream in each unit are equal. The enthalpy temperature path for this type of operation is illustrated in Fig. 2. As is shown, the enthalpy of the desiccant increases in the regenerator at constant temperature. This is associated with increase in the

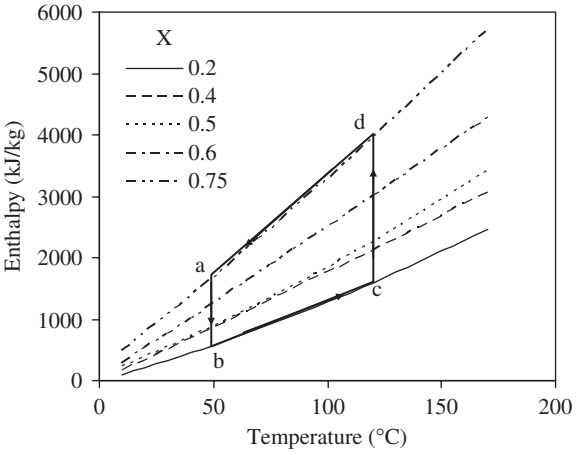

Fig. 2. Variation in the LiBr enthalpy as a function of the boiling temperature and concentration. The points a, b, c, and d correspond to absorber inlet, absorber outlet, desorber inlet, and desorber outlet. X; —, 0.2; --, 0.4; --, 0.5; --, 0.6; --, 0.75.

desiccant concentration. Similarly, the enthalpy of the desiccant in the absorber decreases at constant temperature. It should be noted that the desiccant temperature in the regenerator or absorber are obtained from the equilibrium relation between the water vapor phase and boiling liquid desiccant [22].

Design of the absorption unit includes the water material balance, which is given by

$$M_{ds}(X_{ds_o} - X_{ds_i}) = M_a(W_o - W_h) \tag{19}$$

The absorber energy equation balances the heat generated upon water absorption, latent heat of water vapor condensation, latent heat of water evaporation, heat gained by the feed water stream, and the heat gained by the air stream.

$$M_w C_p(T_{w_f} - T_{w_i}) + M_{d_1}\lambda_{v_1} + M_a(H_{a_o} - H_{a_h}) = M_{d_2}\lambda_{v_2} + M_{ds}(H_{ds_{ai}} - H_{ds_{ao}}) \tag{20}$$

The energy balance of the regeneration unit is given by

$$M_{ds}(H_{ds_o} - H_{ds_i}) + M_{d_2}\lambda_{v_3} = M_s\lambda_s \tag{21}$$

The heat transfer area of the heating steam tubes in the regenerator is given by

$$A_s = \frac{M_s\lambda_s}{U_s(T_s - T_{ds_o})} \tag{22}$$

The energy balance of the condenser unit is given by

$$M_w Cp(T_f - T_{cw}) = M_{d_2}\lambda_{v_3} + M_{d_1}\lambda_{v_1} \tag{23}$$

The heat transfer area of the condenser is given by

$$A_c = \frac{M_{d_2}\lambda_{v_3} + M_{d_1}\lambda_{v_1}}{U_c LMTD_c} \tag{24}$$

The logarithmic mean temperature difference of the condenser is given by

$$LMTD_c = \frac{T_{cw} - T_f}{\ln\left(\frac{T_v - T_f}{T_v - T_{cw}}\right)} \tag{25}$$

The energy balance of the heat exchanger for the diluted/concentrated desiccant is given by

$$M_{ds}(H_{d_o} - H_{a_i}) = (M_{ds} - M_d)(H_{d_i} - H_{a_o}) \tag{26}$$

The heat transfer area of the heat exchanger is given by

$$A_{hx} = \frac{M_{ds}(H_{d_o} - H_{a_i})}{U_{hx}(T_{d_o} - T_{a_i})} \tag{27}$$

Correlations for the lithium bromide enthalpy and the saturation boiling temperature are extracted from reference [22]. An illustration for the system design is made for a production capacity of 1.157 kg/s of fresh water, which corresponds to 100 m^3/d. System temperatures include the inlet air temperature to the humidifier is 25°C, outlet air temperature from the humidifier is 53°C, the outlet air temperature from the absorber unit is equal to the absorber temperature, the intake seawater temperature is equal to 25°C, the outlet seawater temperature leaving the condenser is equal to 50°C, the outlet seawater temperature leaving the absorber and entering the humidifier is equal to 75°C, the outlet seawater temperature leaving the humidifier is equal to 45°C. Other design conditions set the relative humidity of the air stream entering the humidifier at 10%, the relative humidity of the air stream leaving the humidifier at 100%, and the relative humidity of the air stream leaving the absorber at 10%. The tube length and

diameter used in the condenser, regenerator and absorber are equal to 10 and 0.03 m, respectively. The overall heat transfer for the condenser, regenerator, heat exchanger, and absorber are equal to 3, 3, 1 and 3 kW/m^2 K. The overall mass transfer coefficient for water vapor in air is 0.354 kg/s m^3. The mass fraction of lithium bromide in the diluted and concentrated solutions are equal to 0.5 and 0.7, respectively. The vapor temperature in the absorber and regenerator are equal to 53 and 90°C, respectively.

The design results are summarized in Table 3. The summary includes the properties of the air, liquid water, water vapor, and lithium bromide. These properties include the saturation pressure, the absolute humidity, the enthalpy, the latent heat, and the saturation temperature. These results are then used to solve the mass and energy balances as well as the heat transfer equations. This gives the flow rates of the heating steam, desiccant, water, air, and product vapor. Also, the results are used to calculate the height of the humidification tower, and the heat transfer areas in the absorber, regenerator, heat exchanger, and condenser. As is shown, the height of the humidification column is equal to 13.4 m, the performance ratio is equal to 1.37, and the specific heat transfer area is equal to 172.5 m^2/(kg/s). It should be stressed that the performance ratio for this system is higher than, which implies that the amount of product water is larger than the amount of heat steam. Definitely, the results of this illustration do not represent the optimum system performance. Further expanded calculations of the system performance over a wide range of operating parameters is necessary to determine the optimum. Also, such calculations should take into considerations the costing factor.

Table 3
Illustration summary of HDH with desiccant air drying

Property	Value	Units
p_{s_i}	3.169	kPa
p_{s_o}	14.309	kPa
p_{s_c}	46.868	kPa
W_i	0.00195	kg/kg
W_o	0.10229	kg/kg
W_c	0.03017	kg/kg
H_i	30.02	kJ/kg
H_o	313.44	kJ/kg
H_c	154.76	kJ/kg
λ_i	2442.22	kJ/kg
λ_o	2375.31	kJ/kg
λ_c	2309.56	kJ/kg
λ_s	2009.73	kJ/kg
λ_{v_a}	2283.35	kJ/kg
λ_{v_d}	2322.09	kJ/kg
Cp_{a_i}	1.006	kJ/kg K
Cp_{a_o}	1.008	kJ/kg K
Cp_{a_c}	1.011	kJ/kg K
Cp_{c_i}	4.18	kJ/kg K
Cp_{c_o}	4.18	kJ/kg K
Cp_{w_i}	4.19	kJ/kg K
Cp_{w_o}	4.18	kJ/kg K
T_{de_i}	171.4	°C
T_{de_o}	171.4	°C
T_{ab_i}	79.7	°C
T_{ab_o}	79.7	°C
T_s	181.4	°C
H_{ab_i}	2410.9	kJ/kg
H_{ab_o}	1653.9	kJ/kg
H_{de_i}	3565.6	kJ/kg
H_{de_o}	5261.6	kJ/kg
M_s	1.25	kg/s
M_{ds}	2.36	kg/s
M_a	16.05	kg/s
M_w	36.4	kg/s
M_{cw}	25.3	kg/s
A_c	17.1	m^2
$LMTD_c$	51.5	°C
A_{de}	83.7	m^2
A_{hx}	73.2	m^2
A_{ab}	121.6	m^2
$LMTD_{ab}$	13.9	°C
Z_h	13.4	m
M_{d_1}	0.56	kg/s
M_{d_2}	1.16	kg/s
PR	1.37	
sA	172.5	m^2/(kg/s)

5. Humidification membrane drying

The air humidification unit and membrane air drying system is shown in Fig. 1(d). The humidifier characteristics are similar to those in the conventional HDH. This requires heating of the intake seawater to the design temperature. Heating of the intake seawater can be made through the use of a solar collector unit, a diesel engine, saturated steam, or other forms of low grade energy, which might be available in industrial sites. As is shown, the humidified air stream is compressed and passed through the membrane unit. The selective properties of the membrane result in permeation of the air humidity from the feed to the permeate side. As shown in Fig. 1(b), the compressed dried air leaves at the other end of the membrane drying unit. On industrial scale several dehumidification membranes are available for air drying applications. The air compression process would require use of electric power to derive the air compressor motor. On remote locations, this might be possible through the use of photovoltaic cells or wind powered electric generator.

Analysis of this system requires modeling of the intake seawater heater, air humidifier, the humid air compressor, and membrane drying unit. The models for the air humidifier and the intake seawater heater are similar to those in the conventional HDH. The membrane drying model requires definition of the feed conditions and the water vapor permeation constant. A complete mixing model includes molar balances and fluxes of water vapor and air through the membrane. Other model assumption include steady state conditions, constant permeation constants, negligible pressure drop on the permeate and feed sides. Also, the air stream is modeled as a binary system of dry air and water vapor. At steady state conditions, the balance and flux equations are given below

$$Q_f = Q_p + Q_r \tag{28}$$

$$Q_f X_f = Q_p X_p + Q_r X_r \tag{29}$$

$$Q_p X_p = A P_w (p_f X_f - p_p X_p) \tag{30}$$

$$Q_p (1 - X_p) = A P_a (p_f (1 - X_f) - p_p (1 - X_p)) \tag{31}$$

Solution of Eqs. (28–31) requires definition of Q_f, X_f, p_f, p_p, P_w, P_a, and X_p. Simultaneous solution of Eqs. (28–31) results in Q_p, Q_r, X_r, and A. An illustration for design of the membrane separation unit is made for the same design conditions of the HDH system. Therefore, the design data include the following: The feed flow rate of the humidified air leaving the compressor, $Q_f = 6.95$ kg/s, the feed pressure, $p_f = 300$ kPa, the permeate pressure, $p_p = 101$ kpa, the permeance of the water vapor, $P_w = 5.76 \times 10^{-5}$ kg/s kPa, the air permeance, $P_a = 2 \times 10^{-7}$ kg/s kPa, the mass fraction of the water vapor in the feed stream, $X_f = 0.169$, the mass fraction of the water vapor in the reject stream, $X_r = 0.00346$. Simultaneous solution of Eqs. (28–31) gives $A = 397.8$ m^2, $Q_p = 1.177$ kg/s, $Q_r = 5.76$ kg/s, $X_p = 0.98$. These results show more than 90% recovery of the feed water vapor.

6. Conclusions

Four configurations are analyzed for the air humidification dehumidification water desalination system. The configurations include the conventional system, which is formed of an air humidifier and water vapor condenser, the mechanical compressor system, the desiccant system, and the membrane air drying system. Analysis of these of these four configurations show that the main drawback of any air humidification dehumidification system. This is caused by the presence of a large amount of air together with the water

vapor product. Therefore, cooling, compression, condensation, or any other form of air drying will result in processing of the large air stream together with the water vapor product. As a result, the process efficiency is drastically reduced. Also, the required size of a condenser or other drying units will be large. Further evaluation of these configuration is necessary to optimize the unit product cost and to minimize the equipment. This would require detailed design of some special equipment such as the desiccant heat exchanger, the absorber, and regeneration units.

Nomenclature

a — Specific mass transfer area in humidification column, m^2/m^3
A — Area, m^2
Cp — Specific heat at constant pressure, kJ/kg K
h — Heat transfer coefficient, $kW/m^{2\circ}C$.
H — Enthalpy, kJ/kg
k — Thermal conductivity, kW/m K.
Ky — Mass transfer coefficient of water in air, kg/s m^3
$LMTD$ — Logarithmic mean temperature difference, °C
M — Mass flow rate, kg/s p Pressure, kPa
P — Permeance, kg/(m^2 s kPa)
r — Radius, m
Rf — Fouling resistance, $m^{2\circ}C/kW$
T — Temperature, °C
U — Overall heat transfer coefficient, $kW/m^{2\circ}C$
W — Absolute humidity, kg H_2O/kg dry air
x — Mass fraction of desiccant
X — Salinity, ppm
Z — Height of humidification column

Greek Symbols

ϕ — Relative humidity, dimensionless
λ — Latent heat, kJ/kg

Subscripts

a — air
ab — absorber
c — Condenser
cw — Intake seawater
d — Distillate product
ds — Desiccant
f — Feed seawater
h — Humidifier
ht — Heater
hx — Heat exchanger
i — Inlet stream or inner diameter
o — Outlet stream or outer diameter
s — Heating steam or saturation conditions
t — Tube wall
v — Vapor
w — Water

References

[1] K. Bourouni, M. Chaibi and L. Tadrist, Water desalination by humidification and dehumidification of air: state of the art. Desalination, 137 (2001) 167–176.
[2] E. Korngold, E. Korin and I. Ladizhensky, Water desalination by pervaporation with hollow fiber membranes. Desalination, 107 (1996) 121–129.
[3] M.F.A. Goosen, S.S. Sablani, W.H. Shayya, C. Paton and H. Al-Hinai, Thermodynamic and economic consideration in solar desalination. Desalination, 129 (2000) 63–89.
[4] M.A. Younis, M.A. Darwish and F. Juwayhel, Experimental and theoretical study of a humidification-dehumidification desalting system. Desalination, 94 (1993) 11–24.
[5] H. Muller-Holst, M. Engelhardt and W. Scholkopf, Small-scale thermal seawater desalination simulation and optimization of system design. Desalination, 122 (1999) 122–262.

[6] M. Farid and A. Al-Hajaj, Solar desalination with a humidification-dehumidification cycle. Desalination, 106 (1999) 427–429.
[7] S. Al-Hallaj, M.M. Farid and A. Tamimi, Solar desalination with a humidification-dehumidification cycle performance of the unit. Desalination, 120 (1998) 273–280.
[8] N.K. Nawayseh, M.M. Farid, A. Omar, S.M. Al-Hallaj and A. Tamimi, A simulation study to improve the performance of a solar humidification-dehumidification desalination unit constructed in Jordan. Desalination, 109 (1997) 277–284.
[9] N.K. Nawayseh, M.M. Farid, S. Al-Hallaj and A. Al-Timimi, Solar desalination based on humidification process – I. Evaluating the heat and mass transfer coefficients. Energy Conv. Manage., 40 (1999) 1423–1439.
[10] N.K. Nawayseh, M.M. Farid, A. Omar and A. Sabirin, Solar desalination based on humidification process – II. Computer simulation. Energy Conv. Manage., 40 (1999) 1441–1461.
[11] M. Vlachogiannis, V. Bontozoglou, C. Georgalas and G. Litinas, Desalination by mechanical compression of humid air. Desalination, 122 (1999) 35–42.
[12] Y.J. Dai and H.F. Zhang, Experimental investigation of a solar desalination unit with humidification and dehumidification. Desalination, 130 (2000) 169–175.
[13] M.M. Farid, S. Parekh, J.R. Selman and S. Al-Hallaj, Solar desalination with a humidification-dehumidification cycle: mathematical modeling of the unit. Desalination, 151 (2002) 153–164.
[14] H.M. Ettouney, H.T. El-Dessouky and Y. Al-Roumi, Analysis of mechanical vapor compression desalination process. Int. J. Energy Res., 23 (1999) 431–451.
[15] A.S. Foust, L.A. Wenzel, C.W. Clump, L. Maus and L.B. Anderson, Principles of Unit Operations, 2nd ed., John Wiley & Sons, 1980. N.Y.
[16] H.T. El-Desscutey and H.M.Ettovney Fundamentals of Salt Water Desalination, Elsevier, ISBN: 0–444–50810–4, February 2002.
[17] G. Al-Enezi, H.M. Ettouney and N. Fawzi, Low temperature humidification dehumidification desalination process. Energy Conv. Manage., 2005. in print.
[18] S.E. Aly, Vapour compression distillation using waste heat absorption systems. Desalination, 68 (1988) 57–68.
[19] K. Fathalah and S.E. Aly, Theoretical study of a solar powered absorption/MED combined system. Energy Conv., 31 (1991) 529–544.
[20] S. Yanniotis and P.A. Pilavachi, Mathematical modeling and experimental validation of an absorption-driven multiple–effect evaporator. Chem. Eng. Technol., 19 (1996) 448–455.
[21] J. deGunzbourg and D. Larger, Cogeneration applied to very high efficiency thermal seawater desalination plants: a concept. Desalination Water Reuse, 7 (1998) 38–41.
[22] H.M. Hellmann and G. Grossman, Improved property data correlations of absorption fluids for computer simulation of heat pump cycles. ASHRAE Trans Sym., 17 (1996) pp. 980–997.